OPTIMUM PRELOAD RATES FOR COMPRESSIBLE NORMALLY CONSOLIDATED SOILS

RAYMOND J. KRIZEK*, CLARENCE H. C. JAMES**
and
JORJ O. OSTERBERG***

ABSTRACT

The significance of shear strength increases on the allowable preload rate for compressible, normally consolidated soils subjected to a flexible strip load is examined. On the basis of representative soil parameters and various assumed boundary conditions, a computer analysis has been made to systematically predict the rates and magnitudes of shear strength increase and the associated settlements which occur as primary consolidation progresses, and to evaluate the bearing capacity of the soil in terms of these strength increases. Results show that, when adequate drainage is provided, weak soils may be expected to experience a measurable increase in bearing capacity during the consolidation process; furthermore, these increases occur in a time which is compatible with many construction schedules. On the other hand, when drainage is inadequate, slow rates of consolidation preclude the occurrence of any reasonable bearing capacity increase, except for cases where the ratio of the horizontal to the vertical coefficients of consolidation is large. Since consolidation settlement at any given time is governed by the magnitude and duration of the applied load, which is, in turn, governed by the rate of bearing capacity increase, the resulting consolidation settlements can be accelerated to any worthwhile degree only for cases where reasonable bearing capacity increases are experienced. Finally, the benefits of optimizing the preload rate decrease significantly for cases where the initial soil strength is high.

INTRODUCTION

During the past twenty years, there has been an unprecedented growth in federal, state, municipal, and industrial construction. Concomitant with this continuing expansion, the demand for building sites has increased rapidly

* Assoc. Professor, Northwestern University, Evanston, Illinois, U.S.A.
** Assist. Professor, Howard University, Wash., D.C., U.S.A.
*** Professor, Northwestern University, Evanston, Illinois, U.S.A.
Written discussions on this paper should be submitted before April 1, 1970.

and associated land costs have risen accordingly. These conditions make it no longer practical for engineers and builders to avoid the use of marsh lands or tidal flats where the foundation soils consist of weak, plastic, compressible silts, clays, and organic materials. The result has been a growing pressure on soils engineers to make extensive use of precompression as a normal and acceptable means of controlling the magnitude of post-construction settlements under light buildings, oil storage tanks, highway embankments, etc. In addition, there is a growing awareness that advantage can be taken of any strength increase that might occur in the soil during the consolidation process. The purpose of this work is to investigate, by means of a systems approach, (a) the optimum rate at which these soft, compressible soils can be preloaded by taking full advantage of resulting strength increases with time and load, and (b) the consolidation settlements associated with such preload rates.

DESCRIPTION OF PROBLEM

General Considerations

Precompression is a general term which Aldrich (1964) defines as "the deliberate act of compressing the soil under an applied pressure prior to placing or completing the structure load." It is normally accomplished by preloading, which involves the placement and removal of earth, water, or some other dead load to consolidate the soft, compressible foundation soils. The phrase "soft, campressible soils" is used to describe a large number of soil types that respond favorably to preloading techniques, and it includes soft, fine-grained soils which are most often normally consolidated or slightly overconsolidated. Frequently, they are organic silts, fine sands, and occasionally unconsolidated fills, including rubbish fill.

Whenever a load is applied to a soft, compressible soil mass, the induced stresses are reflected initially as excess porewater pressures; as these porewater pressures gradually dissipate, the induced stresses are transferred to the soil skeleton, thereby increasing the soil strength. Hence, the problem of strength increase, as well as consolidation settlement, is a time-dependent one, and the magnitude and or/rate of loading must be controlled in order to avert a bearing capacity failure. The soils engineer is thus faced with the problem of determining, from the standpoint of stability as well as economy, the most favorable combination of load increment and time increment that could be used to achieve the optimum rate of preloading for a given soil. On the one hand, it is desirable to preload as rapidly as possible so as to accelerate the consolidation process and the associated strength gain, whereas, on the other hand, if the preload is applied too rapidly, the required strength gain does not have sufficient time to occur, and a bearing capacity failure will result.

Specific Problem

The specific problem considered herein deals with determining the optimum rate at which a strip load of uniform intensity can be applied to the surface of a soft, saturated, normally consolidated soil overlying a rough, rigid substratum. As previously mentioned, this problem involves the interaction of consolidation settlement and bearing capacity increase, both of which are time dependent. The incentive for studying this problem lies in the basic premise that it is generally desirable to preload at the maximum possible rate.

GENERAL APPROACH

Method of Analysis

The method of analysis employed in this study combines some of the well-known and generally accepted principles of soil mechanics and foundation engineering and utilizes numerical techniques in conjunction with a digital computer to synthesize discrete works found in several individual component problem areas, such as stress distribution, consolidation, effective stress-strength relationship, and bearing capacity determinations. As such, the emphasis is not to advance new theories and/or data, but rather to apply existing knowledge and/or theories to study a practical engineering problem.

The following comments provide a more detailed description of the general approach to this problem. On the basis of a postulated empirical rule describing the variation of shear strength with depth, the bearing capacity of a soft, compressible soil layer of finite depth is calculated; then a uniform strip load equal to this bearing capacity times a load factor is applied to the surface. The load factor is simply that percentage, expressed as a decimal, of the calculated bearing capacity which is applied at any time; in particular, the load factor may be regarded as the reciprocal of the safety factor. With the progress of conslidation, the excess porewater pressures will dissipate, the effective stresses will increase, and consolidation settlements will occur. As a result of the increases in the effective stresses, the shear strength of the soil will increase, and the bearing capacity of the soil will become correspondingly greater. This greater soil bearing capacity will allow the applied load to be increased, thereby increasing the rate of consolidation and the rate of bearing capacity increase. This process of incrementally increasing the applied load is continued until the maximum bearing capacity of the soil is approached. Such a method of analysis involes the following fundamental considerations:

(a) What are the distributions of total stresses and initial excess porewater pressures in the soft layer due to the application of a strip load?

(b) What is the rate at which excess porewater pressures are dissipated?

(c) What is the initial strength distribution with depth in the soft layer?
(d) How is the initial strength distribution in the soft layer altered by the dissipation of excess porewater pressures and the associated increase in effective stresses?
(e) What is the bearing capacity of the soft layer at any instant?
(f) What is the consolidation settlement at the surface of the soft layer at any instant?

Assumptions Employed

The following physical, mathematical, and engineering assumptions are employed in the study:

(a) Darcy's Law is valid, and the time lag of consolidation is due entirely to the low permeabilities of the soil.
(b) The soft, compressible soil is completely saturated.
(c) The Mohr-Coulomb strength theory is valid.
(d) A $\phi = 0$ analysis is valid, and potential failure surfaces are cylindrical in shape.
(e) The initial shear strength distribution obeys a postulated, empirical strength relation.
(f) The problem is one of plane strain.
(g) Although it is recognized that Poisson's ratio for the soil-water matrix may decrease somewhat during consolidation, a constant value of 0.5 is assumed when calculating the intermediate principal stress.
(h) The contact between the base of the load and the soil is rough.
(i) The surcharge has no strength, and each load increment is applied instantaneously.
(j) Initial excess porewater pressures can be expressed in terms of octahedral normal stresses, octahedral shear stresses, and the Skempon (1954) parameters A and B.
(k) All soil properties, except for the coefficients of permeability and consolidation in some cases, are isotropic before, during, and after loading.
(l) The soils are homogeneous with respect to all governing properties, except shear strength and void ratio.
(m) The so-called Rutledge hypothesis" holds for relations between compressive strength and major principal effective stress in the range beyond the preconsolidation pressure of the clay.
(n) The coefficient of consolidation in the horizontal direction is a function of the coefficient of vertical compressibility (Moran *et al.*, 1958).
(o) The coefficient of lateral earth pressure is constant and equal to the "at rest" value.
(p) The Boussinesq relations for a strip load on an elastic half-space give reasonably representative values for stresses inclucecd in a clay layer

of finite depth.

(q) The coefficients of consolidation in the horizontal and vertical directions are intrinsic properties of the soil and are independent of the geometry of loading and the boundary conditions.

(r) The ratio of layer thickness to load width is sufficiently large so that a failure surface will not intersect or touch the hard layer below.

(s) Even though the horizontal and vertical coefficients of permeability, the coefficient of vertical compressibility, and the void ratio of the soil may vary with changes in stress, their combined effect is assumed to maintain the coefficients of consolidation in the horizontal and vertical directions nearly constant over the usual loading increments (Moran *et al.*, 1958).

(t) The load distribution on the surface of the soil layer and the associated total stress distribution in the soil mass are unaffected by the consolidation process.

(u) The groundwater table is at the surface of the compressive soil layer.

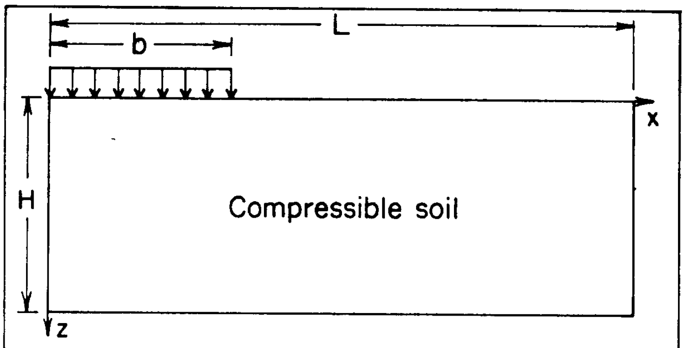

Case	Boundary				
	$x=0$, $0 \le z \le H$	$0 \le x \le b$, $z=0$	$b \le x \le L$, $z=0$	$x=L$, $0 \le z \le H$	$0 \le x \le L$, $z=H$
1	$\frac{\partial u}{\partial x}=0$	$u=0$	$u=0$	$u=0$	$\frac{\partial u}{\partial z}=0$
2	$\frac{\partial u}{\partial x}=0$	$u=0$	$u=0$	$\frac{\partial u}{\partial x}=0$	$\frac{\partial u}{\partial z}=0$
3	$\frac{\partial u}{\partial x}=0$	$\frac{\partial u}{\partial z}=0$	$u=0$	$u=0$	$\frac{\partial u}{\partial z}=0$
4	$\frac{\partial u}{\partial x}=0$	$\frac{\partial u}{\partial z}=0$	$u=0$	$\frac{\partial u}{\partial x}=0$	$\frac{\partial u}{\partial z}=0$
5	$u=0$	$u=0$	$u=0$	$\frac{\partial u}{\partial x}=0$	$\frac{\partial u}{\partial z}=0$

Figure 1. Geometry of problem and boundary conditions considered

(v) Settlements are sufficiently small so that the variation in position of the nodal points in the numerical grid system within the loaded region is negligible.

Boundary Conditions

Analyses have been made for conditions of (a) one-dimensional consolidation with one-dimensional drainage, and (b) one-dimensional consolidation with two-dimensional drainage. Determinations of increases in bearing capacity and consolidation settlements were made for six different sets of boundary conditions; in addition to the one-dimentional drainage case, the five sets of boundary conditions considered for two-dimensional drainage cases are given in Figure 1. Following comparisons of preliminary results, the one-dimensional drainage case and cases 1, 2, and 3 for two-dimensional drainage were eliminated as being of lesser significance, and more detailed analyses were made for the remaining two cases.

THEORETICAL DEVELOPMENT

Postulated Strength Distribution Rule

The evidence gleaned over the years from examination of boring logs has led investigators to subscribe to the hypothesis that, in general, the undrained shear strength, c_u, of a normally consolidated clay increases linearly with depth or with the vertical effective normal stress, p, of the overburden; specifically, the shear strength ratio, c_u/p, is a constant. Accordingly, as shown in Figure 2, the total undrained shear strength, c_t, at a point located a vertical distance, z, below the ground surface may be expressed as

$$c_t(z) = c_0 + (c_u/p)\gamma' z + Fc_0 \exp\left[-(z/\alpha H)^2\right] \quad (1)$$

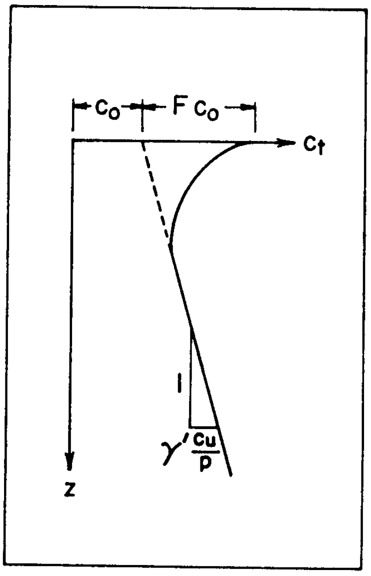

Figure 2. Assumed initial distribution of shear strength with depth

where γ' is the submerged unit weight of the soil, c_0 is the zero intercept on the strength axis of the linear portion of the composite strength curve, and F and α are empirical coefficients, which are discussed subsequently. The empirical coefficients are dimensionless, and the other parameters must be expressed in a consistent set of units. The last term on the right-hand side of equation (1) reflects the condition of greater shear strength in the upper few feet of the clay as a result of overconsolidation due to dessication or fluctuation of the ground-water table. The role of F is to establish a maximum value for c_t at the upper surface of the overconsolidated zone; it is unreasonable to assume too high a value for F because a high degree of overconsolidation at the surface would probably introduce surface cracks and negate the existence of any strength in this region. The coefficient α describes the attenuation rate of the effect of this assumed overconsolidation in the upper zone; practical estimates for α can be obtained by choosing the z/H value at which the strength difference between the curve describing the data and the extended straight-line portion of that curve is approximately equal to one-third of Fc_0.

Bearing Capacity Determination

For a strip load of width, $2b$, applied to the surface of a purely cohesive soil whose undrained strength characteristics are represented by equation (1), the initial or no-load bearing capacity, q_i, based on the assumption of a cylindrical failure surface, can be determined by utilizing a minimization procedure in conjunction with the equilibrium equation. This procedure has been explained in detail by James, Krizek, and Baker (1968) and will not be repeated herein. As consolidation progresses, the soil bearing capacity, designated as q, will change, but the procedure by which it is determined remains the same as indicated above.

Total Stress Distribution

When a load is applied to the surface of a soil mass, there is a measurable total stress increase at all points within a "zone of influence." Based on the assumptions of linear elasticity and plane strain, and referring to the coordinate system shown in Figure 1, we have

$$\tau_{xy} = \tau_{yz} = 0 \tag{2}$$

and

$$\sigma_y = \nu(\sigma_x + \sigma_z) \tag{3}$$

where σ_y is the intermediate principal stress, σ_2, and ν is Poisson's ratio. The induced stresses, σ_x, σ_z, and τ_{xz}, acting at a point in the compressible soil layer, are determined from the elastic solution for a strip load resting on a half-space; although the approximation of a half-space is admittedly in error, it is felt that the nature of the problem under consideration does not demand greater refinement. The total induced stresses at a point within the compressible soil layer may be separated into dilatational and deviatoric components, $[\sigma']$ and $[\sigma'']$, respectively, and written as

$$[\sigma] = [\sigma'] + [\sigma''] = \begin{bmatrix} \sigma_{oct} & 0 & 0 \\ 0 & \sigma_{oct} & 0 \\ 0 & 0 & \sigma_{oct} \end{bmatrix} = \begin{bmatrix} \sigma_x - \sigma_{oct} & 0 & \tau_{xz} \\ 0 & \sigma_y - \sigma_{oct} & 0 \\ \tau_{xz} & 0 & \sigma_z - \sigma_{oct} \end{bmatrix} \tag{4}$$

where

$$\sigma_{oct} = \frac{1}{3}(\sigma_x + \sigma_y + \sigma_z) = \frac{1}{3}[(1 + \nu)(\sigma_x + \sigma_z)] . \tag{5}$$

For subsequent use, we may define

$$\tau_{oct} = \frac{1}{3}\sqrt{(\sigma_x - \sigma_y)^2 + (\sigma_y - \sigma_z)^2 + (\sigma_z - \sigma_x)^2 + 6\tau_{xz}^2} . \tag{6}$$

Initial Excess Porewater Pressure Distribution

The process of consolidation depends upon the rate at which excess porewater pressures are dissipated throughout the soil mass. One very important factor which governs this dissipation process is the initial excess porewater pressure distribution which results immediately after an external load is applied to the soil. There is no general agreement on how this distribution may be represented analytically, but several suggestions have been advanced by Terzaghi (1943), Skempton (1948a, c), Bjerrum (1954), Henkel (1960), and Henkel and Wade (1966). For the work herein, the following relation for the initial excess porewater pressure, u_i, is used:

$$u_i = \sigma_{oct} + a\tau_{oct} \tag{7}$$

where "a" is the Henkel (1960) porewater pressure parameter which is related to the Skempton (1954) A parameter by the relation:

$$\sqrt{2}\,a = A - \frac{1}{3} . \tag{8}$$

Distribution of Excess Porewater Pressure

Immediately following the application of a load to a saturated soil, the induced initial porewater pressures begin to dissipate. Coupled with this dissipation process is the phenomenon of porewater pressure spreading, which results from the comparatively rapid dissipation of porewater pressure at points under the load; unless there is easy access to a drainage face, this porewater is trapped in the regions under the load, and there is a sharp increase in the excess porewater pressure in these zones. Such an increase may remain in evidence for a considerable length of time before a decrease ensues.

A general theory of consolidation, which includes the interrelationship between the stress distribution and the consolidation process, was developed by Biot (1941). Based on this theory, Gibson and Lumb (1953) showed that the consolidation process may be approximately described by the equation:

$$-\frac{\partial \sigma_{oct}}{\partial t} + \frac{\partial u}{\partial t} = C_3\left[\frac{\partial^2 u}{\partial x^2} + \frac{\partial^2 u}{\partial y^2} + \frac{\partial^2 u}{\partial z^2}\right] \tag{9}$$

where C_3 is the three-dimensional coefficient of consolidation. In applying simplifying assumptions to this equation, Davis and Poulos (1968) make a distinction between the application of stresses to a soil specimen in a triaxial consolidation test and the loading of a soil mass in the field. For the case of a laboratory test in which the applied stresses are maintained constant during the consolidation process, the term $\partial\sigma_{oct}/\partial t$ is zero, and equation (9) reduces to the heat conduction equation for which several analytical solutions are available. In problems involving the application of load to a soil mass, the term $\partial\sigma_{oct}/\partial t$ is not generally zero, even when the load is constant; this is because of the stress redistribution which takes place within a three-dimensional soil mass during consolidation. Strictly speaking, equation (9) cannot be solved exactly without recourse to the full theory of Biot. However, in many cases, the overall change in the distribution of σ_{oct} from the start to finish of consolidation is not very great and, as a first approximation, the term $\partial\sigma_{oct}/\partial t$ may be ignored; this, of course, is not permissible when there are changes in total stresses due to changes in the foundation loads with time. For the problem considerd herein, $\partial\sigma_{0ct}/\partial t$ was assumed equal to zero, except for the discontinuity which occurs at the instantaneous application of each increment of load.

For two-dimensional flow in the $x-z$ plane and for anisotropic permeability, the equivalent of equation (9) may be written as

$$c_h\frac{\partial^2 u}{\partial x^2}+c_v\frac{\partial^2 u}{\partial z^2}=\frac{\partial u}{\partial t} \tag{10}$$

where c_h and c_v are the horizontal and vertical coefficients of consolidation, respectively, under two-dimensional drainage conditions. If we let

$$c_h=\eta^2 c_v\,, \tag{11}$$

then equation (10) becomes

$$c_v\left[\eta^2\frac{\partial^2 u}{\partial x^2}+\frac{\partial^2 u}{\partial z^2}\right]=\frac{\partial u}{\partial t}\,. \tag{12}$$

As a special case of equation (12), the differential equation for vertical consolidation and one-dimensional drainage is

$$c_v\frac{\partial^2 u}{\partial z^2}=\frac{\partial u}{\partial t}\,. \tag{13}$$

By use of the normalized variables

$$U=\frac{u}{q_i} \tag{14}$$

$$T = \frac{c_v t}{H^2} \tag{15}$$

$$X = \frac{x}{\eta H} \tag{16}$$

and

$$Z = \frac{z}{H}\,, \tag{17}$$

Equation (12) can be written as

$$\frac{\partial^2 U}{\partial X^2} + \frac{\partial^2 U}{\partial Z^2} = \frac{\partial U}{\partial T}\,. \tag{18}$$

Similarly, equation (13) becomes

$$\frac{\partial^2 U}{\partial Z^2} = \frac{\partial U}{\partial T}\,. \tag{19}$$

Porewater Pressure-Effective Stress Relationship

At any time following the application of a load, decrease in porewater pressure is reflected as an increase in effective stress. With the assumption that each effective stress component is increased by the same percentage that the porewater pressure is decreased (this is consistent with the definition of principal effective stress components; Skempton, 1948b), we can write

$$\left[1 - \frac{u(t)}{u_i}\right]u_i = \bar{\sigma}_{oct} + a\bar{\tau}_{oct} \tag{20}$$

where $u(t)$ is the excess porewater pressure as a function of time. Each increase in each effective stress component is added to the corresponding component of the existing effective stress. In the case of the first load increment, the existing effective stress distribution is generally due only to the overburden stress. For subsequent load increaments, the effective stresses at a point are the respective sums of the initial effective stress components plus all subsequent time-dependent increase in each component.

Effective Stress-Shear Strength Relationship

According to work reported by the United States Army Engineer Waterways Experiment Station (1944), there is, for saturated, normally consolidated, undisturbed clays, a unique relationship between the water content at the end of a triaxial test and the compressive strength, irrespective of the value of the minor principal stress or of the test method. In addition, there is a unique relationship between water content and major principal effective stress, $\bar{\sigma}_1$, in the compression range beyond the preconsolidation pressure,

p_c. Since void ratio, e, and water content, w, are uniquely related for a saturated soil, for all values of $\bar{\sigma}_1$, equal to or greater than p_c, the slopes of the $e-\log\bar{\sigma}_1$ and the $e-\log s$ curves are essentially parallel. These findings, often termed the "Rutledge hypothesis," were later confirmed through investigations conducted on both undisturbed and remolded clays (Bjerrum, 1954). The results of tests carried to failure on normally consolidated samples of Weald and London clays (Henkel, 1960) also conform to this pattern. Although various other effective stress-shear strength relationships have been reported (Skempton, 1948a; Henkel and Wade, 1966), the one described above has been used in this study.

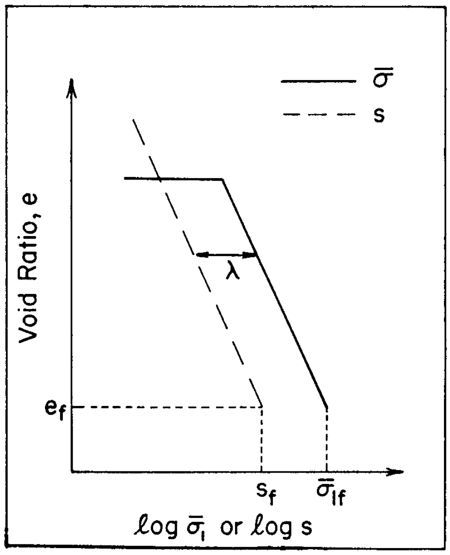

Figure 3. Shear strength-effective stress relationship

As shown in Figure 3, the constant, λ, defined as the Rutledge strength parameter, is the horizontal distance between the two curves described; the associated algebraic relationship between the shear strength, s, and the major principal effective stress, $\bar{\sigma}_1$, may be developed as follows. From Figure 3, we have

$$e=\log\bar{\sigma}+R_\sigma \tag{21}$$

and

$$e=\log s+R_s \tag{22}$$

where R_σ and R_s are constants to be determined. At e equal to e_f, $\bar{\sigma}_1$ equals $\bar{\sigma}_{1f}$ and s equals s_f, where the subscript "f" refers to some final condition. Use of these conditions in conjunction with equations (21) and (22) allows us to write

$$\lambda=\frac{s_f}{\bar{\sigma}_{1f}}=\frac{s}{\bar{\sigma}_1} \tag{23}$$

where λ usually lies in the range between 0.2 and 0.6.

Consolidation Settlement

The determination of consolidation settlements in the compressible soil layer involves the following assumptions in addition to those already stated.

(a) The $e-\log\bar{\sigma}_1$ relationship can be expressed by the idealized curve shown in Figure 3.

(b) The initial overburden or preconsolidation pressure, p_c, anywhere in the soil mass satisfies the empirical relation

$$p_c = \gamma' z + p_0 \exp\left[-(z/\alpha H)^2\right] \tag{24}$$

where p_0 is defined as the stress overconsolidation coefficient and α is the same as previously defined. For normally consolidated soils, some slight overconsolidation due to dessication may exist in the upper few feet, but it is felt that the magnitude of these shrinkage stresses would not become very large before cracks would develop. From a mathematical point of view, equation (24) must not be zero; otherwise the change in void ratio or decrease in volume will be infinite. As a consequence, a p_0 value of 100 psf has been chosen for this study.

(c) One point on an $e-\log\bar{\sigma}_1$ curve for a sample from beneath the proposed loaded area is sufficient to determine the initial void ratio, e_0, at any point under the load.

(d) There is no deflection at the base of the compressible layer (*i.e.*, at the upper surface of the firm layer).

From the basic phase diagram depicting the various components in a soil mass, the relationship between change in void ratio and change in height may be written as

$$\frac{\Delta e}{1+e_0} = \frac{\Delta H}{H} \tag{25}$$

where $1+e_0$ and Δe are the original thickness and the change in void ratio of a two-phase sample, and H and ΔH are the original thickness and the change in thickness of the clay layer, respectively. For a given increase in effective stress beyond the preconsolidation stress, we have

$$\frac{\Delta H}{H} = \frac{C_c}{1+e_0}\log\frac{\bar{\sigma}}{p_c} \tag{26}$$

where C_c is the compression index of the compressible soil.

METHOD OF SOLUTION

Numerical Procedure

Equation (18) was written in terms of finite differences and solved for the boundary conditions stated in Figure 1. The artificial boundary specified by $x=L$ and $0\leqq z\leqq H$ was carefully studied, both with respect to its location and with respect to the assigned boundary condition, to determine its effect on the computed results. The conclusions were (a) that a distance, L, of approximately 4b is adequate in order to neglect the influence of the boundary, and (b) that consideration of this boundary as impermeable ($\partial u/\partial x = 0$) or free ($u=0$) had no significant effect; hence, the cases corresponding to 4 and 5 in Figure 1 were solved for $L \cong 4$b, where the exact value for L depends on η. In order to enhance the stability of the solution, the time increment was taken as either 0.1 or 0.05 times the square of the space increment. A similar method of solution was applied to equation (19), except that the ratio of time increment to square of the space increment was 1/6 and the artificial boundary played no role in the solution. After a few preliminary solutions to equation (19), this case was discarded in favor of the more realistic conditions specified by equation (18) and the boundary conditions stated in cases 4 and 5.

According to this method of solution, the behavior of the soil mass is determined at a finite number of discrete nodal points; if values of a given parameter, such as shear strength, are desired at points intermediate to the nodal points, linear interpolation is employed. Bearing capacity determinations were made after an arbitrarily specified number (100 in most cases) of time increments, and the load was increased instantaneously to a magnitude compatible with the new bearing capacity times a load factor. For a typical clay layer as considered herein, the time factor, T, should be much less than unity in order to operate within a realistic field precompression time; with this in mind, and equally important, in the interest of economy of computer time, it was decided that a minimum of 3 percent increase in bearing capacity would be acceptable for a given number of time cycles. An increase in q of less than 1 percent over the previous q value was used as the criterion for terminating the computer solution. The consolidation settlement between two successive nodal points is algebraically determined by using equations (25) and (26), and total settlement along a grid line is determined by a summation procedure. Additional details regarding the method of solution have been reported by James (1968).

Computer program

The described method of solution necessitates two basic computer programs, one for determining the bearing capacity and one for determining the consolidation settlement and bearing capacity increase. The procedure for the bearing capacity determination has been reported by James, Krizek, and Baker (1968) and will not be repeated herein. A flow diagram of procedures followed in determining the consolidation settlement and the bearing capacity increase is shown in Figure 4. This sequence may be described in greater detail as follows:

(a) Enter the main program, apply the initial load to the soil surface, and compute the total induced stresses and the initial porewater pressures at all nodal points.

(b) Enter the settlement subroutine and compute e_0 and p_c at all nodal points.

(c) Enter the porewater pressure subroutine, and, for a given time factor

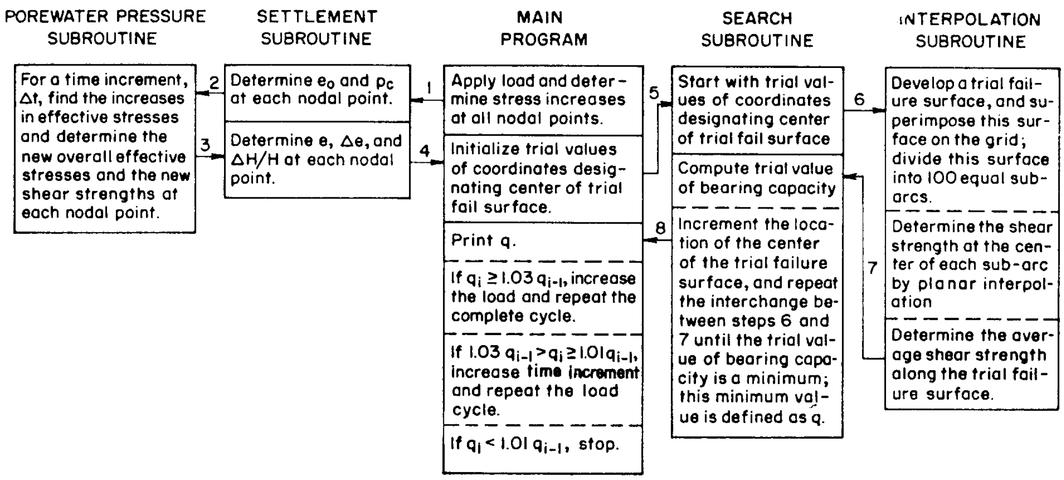

Figure 4. Flow diagram of procedures for determining bearing capacity increase and consolidation settlement under step loading.

increment, ΔT, find the percent dissipation of porewater pressure and the resulting increase in effective stresses at each nodal point; to the effective stresses that existed at the beginning of the time increment and corresponding components of the principal effective stress increments.

(d) Use the effective stress-strength relationship to determine new shear strengths.

(e) Reenter the settlement subroutine and, with the major principal effective stresses now known, calculate the new void ratio, e, the change in void ratio, Δe, and the settlement ratio, $\Delta H/H$, at all points under the load.

(f) Reenter the main program, and initialize trial values of coordinates which specify the center of the trial failure surface.

(g) Enter the search subroutine, and initialize those same coordinates.

(h) Enter the interpolation subroutine with the above coordinates, develop a trial failure surface, and superimpose the failure surface on the strength grid; divide the failure arc into 100 equal sub-arcs, determine the strength at the center point of each sub-arc by planar interpolation in the strength grid, and calculate the average shear strength along the potential failure surface.

(i) Reenter the search subroutine and compute a trial bearing capacity; increment the coordinates designating the center of the failure surface and repeat the interchange between steps 6 and 7 in Figure 4 until q is minimized.

(j) Reenter the main program and print q; take the difference between the new q and the old, multiply this difference by the assigned load factor, and increase the preceding load by this amount.

(k) Repeat all pertinent steps in the entire sequence of procedures, and continue to repeat this cycle as long as the bearing capacity of the soil continues to increase at some minimum specified rate with time and with increasing load.

RESULTS

Selection of Parameters

In order to select input parameters which are representative of the soil types considered herein, an extensive study of the literature was conducted, and some of the results are summarized in Tables 1, 2, and 3. Based on this study, the ranges of values shown in Table 4 were selected as being reasonable for the problems under study; in addition, a so-called reference problem has been defined by the values shown in Table 4, and variations from this reference problem were made by varying only one of the indicated parameters.

Bearing Capacity Increase and Consolidation Settlement

Because of the large number of parameters and the multi-valued nature

Table 1. Average values

C_c	e_0	e at $\bar{\sigma}_1=2000$ psf	c_v (ft^2/day)	w_h	w_{LL}	I_P
0.57	1.96	1.38	0.007	74	81	50
0.44	1.26	1.26	0.03		74.4	47
0.40	1.52	1.31	0.14		58.5	23
0.67	2.05	1.72	0.008	66	60 to 80	30 to 50
0.64	1.42	1.42	0.23	51.5	49.5	19
0.61	1.555	1.555	0.28	54	49.5	19
0.57	1.47	1.37		54	55.5	29.5
0.95	2.2	1.83	0.03-0.2	84	84	38
0.21	1.21	0.76			61	43
0.42	1.65	1.01			61	43
0.46			0.67, $p>p_c$ 0.17, $p<p_c$	47	67	39
1.0			0.02	89		
2.5			0.3	228 to 1000		
			0.16-0.39	40 to 184		
(0.6 to 0.9)			0.05	60 to 80	50 to 65	25 to 35
			[2.6 and 4.4]	30 to 50	30 to 60	
(0.55 to 1.12)			0.042	85	100	61

of the majority of them, a comprehensive quantitative treatment of this problem is not feasible; rather, it is reasonable to treat only a judicious selection of combinations which will typically evaluate the relationships among loading rate, rate of consolidation settlement, and rate of increase in bearing capacity. As previously indicated, problems with two particular sets of boundary conditions are treated in detail; these are stated as cases 4 and 5 in Figure 1 and are designated hereafter as the no-edge-drain case and the edge-drain case, respectively, The only difference between the two sets of boundary conditions lies in the drainage conditions under the load.

For the one-dimensional drainage case, even with the maximum load factor of unity, the increase in bearing capacity was less than 1 percent at $T=0.157$ (*i.e.*, after the first 100 time cycles) and less than 2.5 percent at T equal to 0.3; hence, as previously mentioned, results based on one-dimensional drainage are not considered further in this study. For the two-dimensional drainage, no-edge-drain case with a load factor equal to unity, results showed that no significant increase in bearing capacity occurred for T values as high as 0.3, except when η^2 was taken equal to 4; in this instance, q

of soil properties

G	p_c (psf)	Type of Deposit	Reference
2.67		Normally consolidated clay, from Gosport, UK	Skempton, 1948c
2.7		Plastic blue clay	Osterberg, 1965
2.77	1000	Organic silt (OH)	Lowe *et al*, 1964
		CH	Sowers, 1964
	5000	Soft gray organic silt	Moran *et al*, 1958
	5000	Soft gray organic silt	Moran *et al*, 1958
2.71		Soft Chicago clay	U.S.W.E.S., 1944
2.61	1000	Organic clay (average values from several e-log $\bar{\sigma}_1$ curves)	Schmidt and Gould, 1968
2.76		Zurich tile clay (14% clay fraction)	Bjerrum, 1954
2.70		Allschwyll tile clay (OH)	Bjerrum, 1954
		Blue-gray inorganic silty clay, California	Moran *et al*, 1958
		Bay mud, California	Moran *et al*, 1958
		Fibrous peat	Moran *et al*, 1958
		Soft organic silty clay	Moran *et al*, 1958
	540	Bay mud, 50-70% clay	Moran *et al*, 1958
		40ft of organic silt and organic silty clay, Ill.	Moran *et al*, 1958
		Organic silty claty	Jonas, 1964

Table 2, Typical values of c_0 and c_u/p

c_0 (psf)	$\frac{c_u}{p}$	Soil Type	Reference
300	0.19	Grey silty clay with sand and gravel Cleveland, Ohio	Wu, 1960; Figure 9
120	0.227	Organic silty clay; tidal marsh San Juan, Puerto Rico	Jonas, 1964; Figure 3
320	0.23	Sensitive marine clay Quebec, Canada	Brown and Paterson, 1964; Figure 2
200	(0.12 to 0.22)	Grey, silty clay Detroit, Michigan	Wu, 1960; Figure 3
400	0.15	Grey sily, clay with sand Saginaw, Michigan	Wu, 1960; Figure 4
500	(0.09 to 0.13)	Red clay with grey silt lenses Sault Ste. Marie, Canada	Wu, 1960; Figure 5
240	0.27	Black and grey clay and fill Gosport, United Kingdom	Skempton, 1948c; Figure 3,4,5
200		Clay with layers of fine sand, Sweden	Carlson, 1948; Figure 8
400		Firm brown clay underlain by mottled clay Kippen, Sweden	Bishop and Bjerrum, 1960; Figure 16
100	0.16	Drammen clay; Norway	Simons, 1960; Figure 2
220		Dark, inorganic clay and green silty clay LaSalle, Illinois	Moran *et al*, 1958; Plate Illinois 2.1-2

Table 3. Values of effective stress-strength parameter

λ	Clay Type	Reference
0.4	Plastic blue clay	Osterberg, 1965
0.2	Drammen clay	Bjerrum, 1967
0.27	Bannalp clay	Bjerrum, 1954
0.28	Zurich tile clay	Bjerrum, 1954
0.5	Minnesota clay	Lambe, 1951
0.66	Massena clay	U.S.W.E.S., 1944
0.5	Soft Chicago clay	U.S.W.E.S., 1944
0.3	Zurich talus clay	Bjerum, 1954
0.3	Uetliberg clay	Bjerum, 1954

increased by 29 percent at T equal to 0.97. For the two-dimensional drainage, edge-drain case, there were early increases in bearning capacity followed by perceptibly decreasing rates of increase. Figures 5, 6, and 7 show typical results for some of the cases considered and indicate in a general manner how the various soil parameters influence the rate and magnitude of bearing capacity increase and consolidation settlement.

Figure 5 shows a comparison of the rate and magnitude of increase in q for the edge-drain and no-edge-drain cases when η^2 equals 4; the effect of adequate drainage surfaces is evident. Even though a 29 percent or

Table 4. Range of values for parameters under study

Parameter	Units	Range Selected	Reference Problem
c_0	psf	100 to 600	200
c_u/p		0 to 0.3	0.1
F		0 to 4	1
α		0.2 to 0.32	0.08
λ		0.2 to 0.6	0.4
C_c		0.2 to 1.0	0.6
γ_t	pcf	90 to 120	100
H	ft	20 to 50	30
b/H		0.2 to 0.8	0.6
η^2		1 to 8	1
A		0.5 to 1	1
B		0.9 to 1	1
$\bar{\sigma}_1$	psf		2000
$e(\bar{\sigma}_1)$		0.75 to 2.0	1.4
p_0	psf	100 to 2000	100
K_0		0.5 to 0.6	0.6

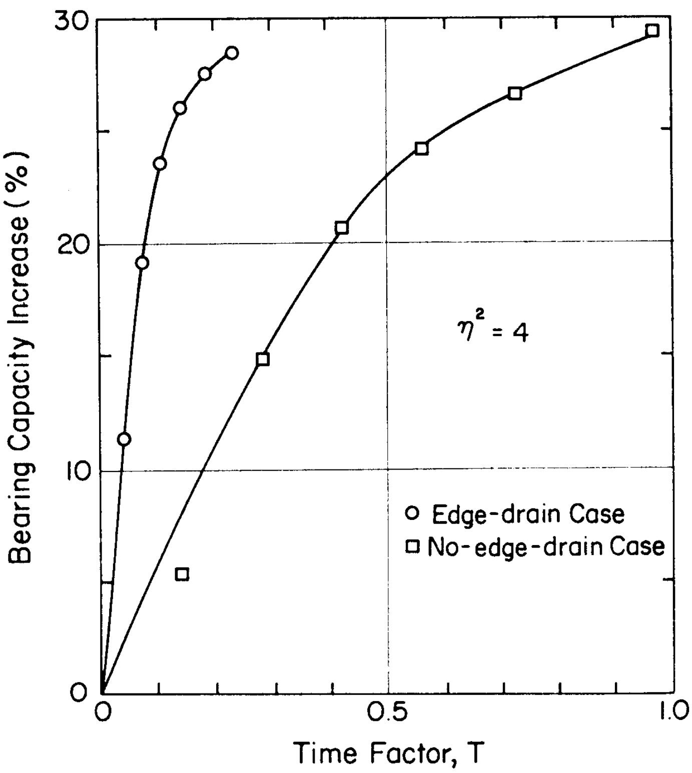

Figure 5. Comparative rates of bearing capacity increase for different boundary conditions

larger increase is achieved for the no-edge-drain case, the time required is quite large, and in all probability will not be compatible with the average field construction schedule. Comparison of the two curves shows that the time required for a given increase in q for the no-edge-drain case is about 4 to 6 times that required for the edge-drain case.

Figure 6a shows bearing capacity increase as a function of load factor

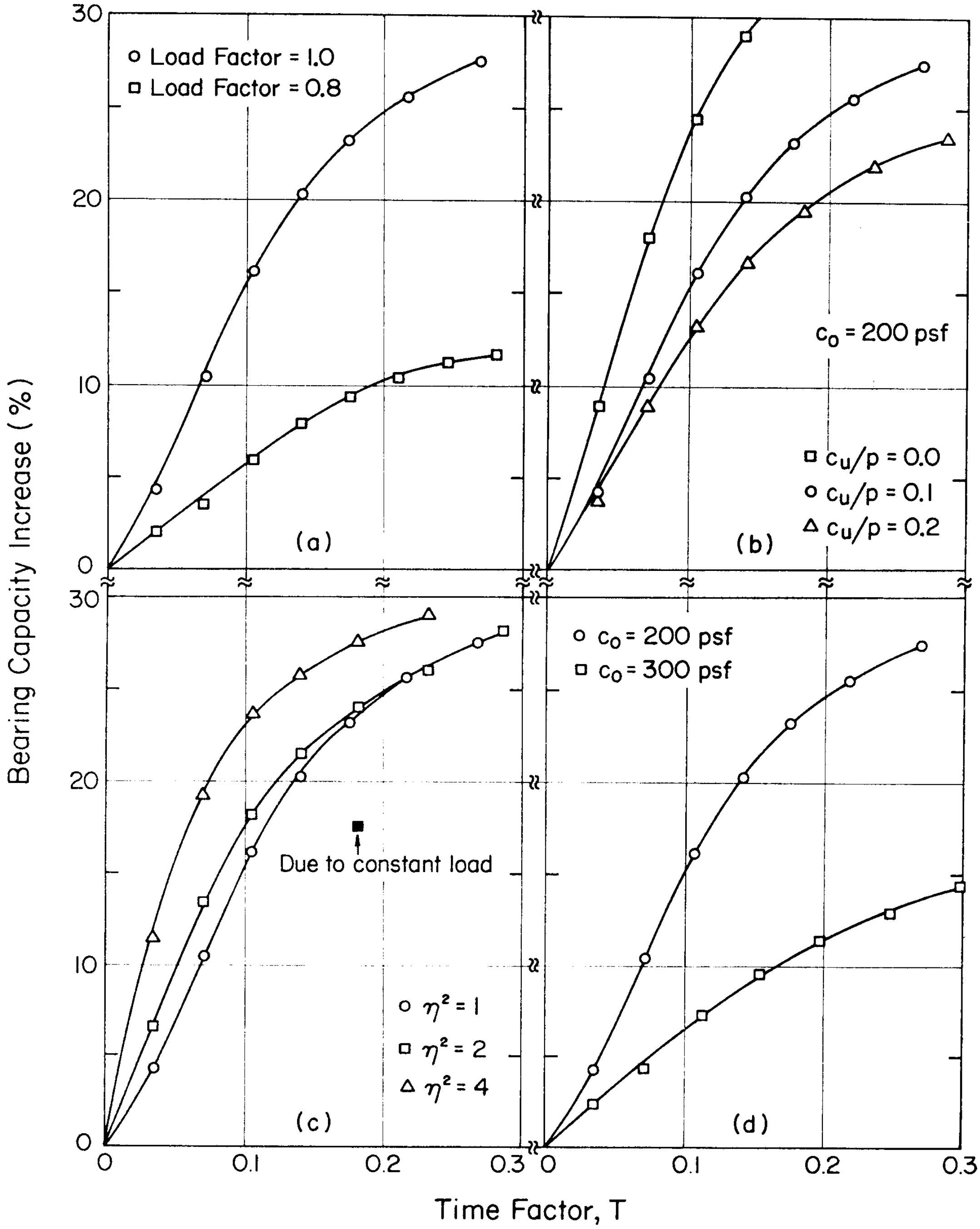

Figure 6. Representative cases of bearing capacity increase

for load factors of 0.8 and 1.0. For a load factor of unity, the rate and magnitude of increase in q are significantly higher than for a load factor of 0.8; also, the consolidation settlement shown in Figure 7a is larger in magnitude and rate. Results of this study indicate that, from a practical point of view, load factors less than 0.8 (or safety factors greater than 1.25) are ineffective for achieving a significant bearing capacity increase in a reasonable period of time; therefore, all other results reported herein employ a load factor of unity. As a consequence, the increase in applied load is equal to the bearing capacity increase, and the discrete points shown in Figure 6 actually represent the increase in applied load or preload rate. Figure 6b shows relative values of q for different values of c_u/p. The largest percentage increase and the fastest rate of increase in q occur in the weakest soil; however, a word of caution must be introduced concerning the literal interpretation of the three curves. Based on the strength distribution rule given by equation (1), the bearing capacity of the soil with the lowest c_u/p ratio will tend to increase at a faster rate, even though the final maximum value may well be smallest for the weakest soil.

Figure 6c shows that the rate of increase of q increases somewhat with increasing values of η^2; the curves show also that, as T approaches 0.3, the increase in q approaches the same maximum value for all η^2. For the case where $\eta^2=2$, Figure 6c also shows the increase in bearing capacity with time for two modes of loading, the constant load and the step load. The single point represents the bearing capacity increase which occurs under a constant load applied from zero time to a time equivalent to the sum of time increments required to complete five step load increments. Although the difference between the respective bearing capacity increase is relatively small (about 9 percent at T equal to 0.182), the time required to achieve a given increase (say 15.5 per cent) occurs for the step load procedure in about one-half the time required for the constant load procedure. The settlement-time relations in Figure 7b show that at a given time the settlement under a constant load is less than under the step load. Although, at T equal to 0.182, the differences in the consolidation settlements under the edge and under the center of the load due to the different loading procedures is only about 10 and 6 percent, respectively the same amount of settlement occurs in about half the time when the step load procedure is employed. These results can be used to advantage, particularly for soils with high coefficients of secondary compression, since Moran *et al.* (1958), Leonards and Ramiah (1959), and others have shown that even moderate surcharges can significantly reduce the effects of post-construction secondary compression.

Figure 7c shows a comparison of the trends in consolidation settlements for the edge-drain and no-edge-drain cases when η^2 equals 4; again the effect of adequate drainage surfaces can readily be appreciated. For example, a given settlement of 0.125 H under the center of the load is accomplished for the edge-drain case in about one-tenth of the time required for the no-edge-drain case. In Figure 7d rates of consolidation settlement are compared for cases in which η^2 equals 1 and 4; these results indicate the effect caused by anisotropic permeability or silt (sand) seams when k_h is greater than k_v. Figure 6d indicates relative rates of increase in bearing capacity as a function of the initial shear strength intercept, c_0. The decrease in the rate of bearing capacity increase for the higher value of c_0 is evident, and it may be inferred that the probable maximum bearing capacity increase also will decrease as c_0 increases.

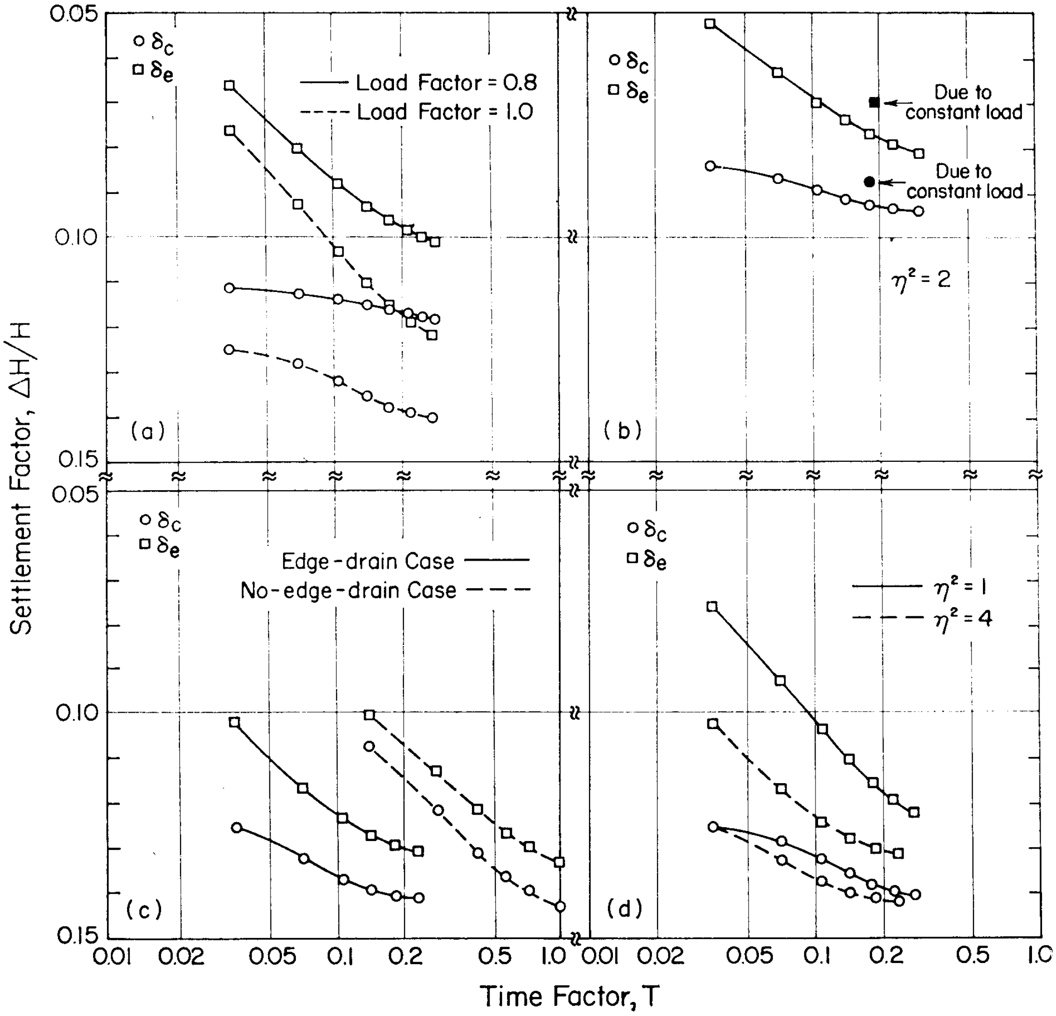

Figure 7. Representative cases of consolidation settlement

CONCLUSIONS

On the basis of a limited digital computer study of the behavior of normally consolidated, soft clay soils under a flexible strip load of uniform intensity, the following conclusions may be drawn.

(a) One of the chief requirements for effectively optimizing the preload rate of a soft soil is the provision of adequate drainage surfaces. For the case of two-dimensional drainage with no edge drains or blanket, slow rates of consolidation result in slow rates of strength increase; thus, there is no appreciable gain in ultimate bearing capacity except when the consolidation coefficient ratio is large. On the other hand; noticeable increases occur in the edge-drain problem under most of the conditions investigated.

(b) Although the rates of consolidation settlement and bearing capacity increase are higher under the step preload procedure than when a constant preload is used, the magnitude, after a given time interval, of both the consolidation settlement and bearing capacity increase may not be significantly greater under step loading.

(c) If the undrained shear strength is a function of depth, the bearing capacity becomes a function of the width of the proposed surface load.

(d) During the loading and consolidation process, the rate of bearing capacity increase varies approximately directly as the consolidation coefficient ratio until the maximum possible value of bearing capacity is approached.

(e) For given values of the consolidation coefficient ratio and the load factor, the rate and magnitude of bearing capacity increase tend to decrease with increasing values of the c_u/p ratio.

(f) The manitude of bearing capacity increase decreases with increasing values of initial strength; thus, the benefit of precompression for purposes of increasing the bearing capacity of a soil decreases with increasing stiffness of the soil.

(g) For the boundary conditions assumed, the ratio of the settlement under the edge of the load to the settlement under the center of the load tends to increase with time, and finally approaches constant value.

Although this entire investigation has been based on the assumption that a strip load is applied to a soil surface, the failure mechanism is fundamentally the same for many different types of surface loads with only a difference in the shape and position of the failure surface. Hence, it seems reasonable to extrapolate these results qualitatively to include other shapes of loaded area.

REFERENCES

Aldrich, H. P., 1964. Precompression for support of shallow foundations. *Proceedings* of the Conference on Design of Foundations for Control of Settlement, ASCE, Evanston, Illinois, 471-506.

Biot, M. A., 1941. General theory of consolidation. *Journal of Applied Physics* 12, 2: 155-164.

Bishop, A. W., and Bjerrum, L., 1960. The relevance of the triaxial test to the solution of stability problems. *Proceedings* of the Research Conference on Shear Strength of Cohesive Soils, ASCE, Boulder, Colorado, 437-501.

Bjerrum, L., 1954. Theoretical and experimental investigations on the shear strength of soils. Norwegian Geotechnical Institute, Publication Number 5.

Bjerrum, L., 1967. Seventh Rankine lecture: Engineering geology of normally consolidated marine clays as related to the settlements of buildings. *Geotechnique* 17, 2: 83-118.

Brown, J., and Prterson, W., 1964. Failure of an oil storage tank founded on a sensitive marine clay. *Canadian Geotecnical Journal* 1, 4: 205-214.

Carlson, L., 1948. Determination *in-situ* of the shear strength of undisturbed clay by means of a rotating auger. *Proceedings* of the Second International Conference on Soil Mechanics and Foundation Engineering, Rotterdam, 265-270.

Davis, E., and Poulos, H., 1968. Three-dimensional rates of consolidation. Preprint of paper and notes from a lecture at a Joint Soil Mechanics Colloquium, University of Illinois' Chicago Circle Campus, Chicago, Illinois, May 22.

Gibson, R., and Lumb, P., 1953. Numerical solution of some problems in the consolidation of clay. *Geotechnique* 2: 182-198.

Henkel, D. J., 1960. The shear strength of saturated remolded clays. *Proceedings* of the Research Conference on Shear Strength of Cohesive Soils, ASCE, Boulder, Colorado, 533-554.

Henkel, D. J., and Wade, N., 1966. Plane strain tests on a saturated remolded clay. Journal of the Soil Mechanics and Foundations Division, ASCE, 92, SM6: 67-80.

James, C. H. C., 1968. Optimum preload rates for compressible normally consolidated soils. Ph. D. Dissertation, Department of Civil Engineering, The Technological Institute, Northwestern University, Evanston, Illinois.

James, C. H. C., Krizek, R. J., and Baker, W. H., 1968. Bearing capacity of purely cohesive soils with a nonhomogeneous strength distribution. Technical Report, Department of Civil Engineering, The Technological Institute, Northwestern University, Evanston, Illinois.

Jonas, E., 1964. Subsurface stabilization of organic silty clay by precompression. *Proceedings* of the Conference on Design of Foundations for Control of Settlement, ASCE, Evanston, Illinois, 447-470.

Lambe, T. W., 1951. Soil testing for engineers. John Wiley and Sons, Inc., New York.

Leonards, G., and Ramiah, B., 1959. Time effects in the consolidation of clays. ASTM, STP Number 254: 116-130.

Lowe, J., Zaccheo, P., and Feldman, H., 1964. Consolidation testing with back pressure. *Proceedings* of the Conference on Design of Foundations for the Control of Settlement, ASCE, Evanston, Illinois, 73-90.

Moran, Proctor, Mueser, and Rutledge, 1958. Study of deep soil stabilization by vertical sand drains. Bureau of Yards and Docks, U.S. Department of the Navy, Washington, D.C.

Osterberg, J. O., 1965. Personal communication.

Schmidt, T., and Gould, J., 1968. Consolidation properties of an organic clay determined from field observations. Preprint of paper presented at the Forty-seventh Annual Meeting of the Highway Research Board, Washington, D. C.

Simons, N. E., 1960. Comprehensive investigations of the shear strength of an undisturbed Drammen clay. *Proceedings* of the Research Conference on Shear Strength of Cohesive Soils, ASCE, Boulder, Colorado, 727-745.

Skempton, A. W., 1948a. A study of the immediate triaxial test on cohesive soils. *Proceedings* of the Second International Conference on Soil Mechanics and Foundation Engineering, Rotterdam, 1: 192-196.

Skempton, A. W., 1948b. The effective stresses in saturated clays strained at constant volume. *Proceedings* of the Seventh International Congress for Applied Mechanics 1: 378-392.

Skempton, A. W., 1948c. The geotechnical properties of a deep stratum of post glacial clay at Gosport. *Proceedings* of the Second International conference on Soil Mechanics and Foundation Engineering, Rotterdam, 1: 145-150.

Skempton, A. W., 1954. The pore-pressure coefficients A and B. *Geotechnique* 4, 4: 143-147.

Sowers, G. F., 1964. Fill settlement in spite of vertical sand drains. *Proceedings* of the Conference on Design of Foundations for the Control of Settlement, ASCE, Evanston, Illinois, 363-376.

U. S. Army Engineers, Waterways Experiment Station, 1944. Review of the cooperative triaxial research program. Prepared by P. C. Rutledge, Vicksburg, Mississippi (published as part of a Comprehensive Report in 1947).

Wu, T. H., 1960. Geotechnical properties of glacial lake clays. Transactions of the American Society of Civil Engineers, 125: 994-1012.

(Received: April 21, 1969)